Parametric study of soft pneumatic robot grippers through finite element analysis

Riady S. Jo[1,2], Evans Ngu[1]
[1]School of Engineering and Physical Sciences, Heriot-Watt University Malaysia, Putrajaya, Malaysia
[2]School of Engineering and Technology, Sunway University, Selangor, Malaysia

Article Info	ABSTRACT
	This paper investigates the gripping stress and deformation of pneumatically-actuated fluidic elastomer actuation (FEA)-based soft robotic gripper through ansys finite element analysis software. By varying gripper parameters, i.e. Input pressures and clearance to the object, simulations on the deformation of the soft fingers are performed to achieve gripping of the object. The motivation of this parametric study is to facilitate the design optimization of soft robotic grippers. Results demonstrate that grippers with lesser clearance to the object require lesser input pressure to achieve similar gripping stress on the object although it is evident that grippers with higher clearance are able to cater for wider range of object sizes.

Corresponding Author:

Riady S. Jo
School of Engineering and Physical Sciences, Heriot-Watt University
Malaysia, Putrajaya, Malaysia
School of Engineering and Technology, Sunway University
Selangor, Malaysia
Email: riadyj@sunway.edu.my

1. INTRODUCTION

Robotic grippers belong to a class of end-effectors that are used primarily in industrial robot applications, ranging from manufacturing, assembly to packaging and sorting of objects. The first electrically-controllable robotic gripper was developed in 1969 by Victor Scheinman as part of the Stanford Arm industrial robot, which tackled the limitations of controlling hydraulic actuation at the time [1]. Since then, many innovations have been made on robotic gripper designs, which conventionally are made of rigid materials and joints.

Traditionally, selections of robot grippers are contingent upon the shapes, sizes, weight and rigidity of the objects to be grasped. This limits the flexibility of re-purposing the robots for different tasks or handling different objects. While robotic grippers eventually gained wide applications in manufacturing industries, the rising applications of robotics and internet of things (IoT) technologies in more sensitive fields, such as agriculture [2]–[4] or food packaging and handling [5]–[7], call for developments of versatile and adaptable robot gripper solutions.

A pioneering work by [8] opened a new sub-field in robotics, where the first shape-adaptable gripper was developed using sets of pulleys and finger segments. Although the segments used were rigid, combining multiple finger segments improved the compliance of the gripper. The success of this work gave birth to the field of soft robotics.

By harnessing the advancement of material engineering, researchers seek to develop a universal robotic gripper that is versatile, highly compliant, adaptable and easily controlled. A comprehensive review of soft robotic grippers was conducted by [9] who proposed a systematic categorization of grasping technologies of soft robot grippers, which in general are: i) gripping by actuation, ii) gripping by controlled stiffness, and iii) grasping by controlled adhesion. Gripping by controlled stiffness manipulate the gripper's overall stiffness that is best used to grasp objects that generally have non-convex shapes. Here, the gripper approaches the object in low stiffness state and in the proximity of the object, the gripper's stiffness is increased to sufficiently grip the object. Some relevant techniques in controlled stiffness gripping includes jamming of granular materials [10]–[14] and manipulating stiffness of shape memory alloys [15]–[17].

Grasping by controlled adhesion is most suitable for grasping flat or deformable objects and the grasping motion is realized by "sticking onto" the object either by effectively changing the friction between surfaces [18]–[21] or through electrostatic adhesion [22],[23]. Soft gripping by actuation is perhaps the most common type of soft gripping category as it extends from conventional gripping that utilizes electromechanical (through electric motors), hydraulic or pneumatic actuation. By definition, the work by [8] therefore belongs to this category.

Recently, soft robotic grippers based on fluidic elastomer actuator (FEA) [24]–[27] have been commonly studied and applied in industrial settings due to the ease of retrofitting them to existing industrial robots. Most FEA-type grippers are actuated by supplying hydraulic or pneumatic pressure to the internal structure of the gripper fingers. The application of pressure deforms the gripper fingers and when several fingers are actuated concurrently, it produces gripping motions.

Despite the many successful developments of FEA-type grippers, in order to optimize future designs, the effect of parameters such as spacing of fingers and input pressures in relation to the objects are yet to be investigated. To this end, this paper investigates the gripping stress and deformation of a FEA-type soft gripper, in particular, a pneumatically-actuated soft gripper through finite element analysis on Ansys. Furthermore, the effect of finger spacing is investigated in relation to the clearance to the gripped object.

2.   PROPOSED MECHANICAL SYSTEM FOR ANSYS SIMULATION
2.1.   Experimental setup

The mechanical design of the soft gripper is shown in Figure 1, and consists of three soft fingers and an end-effector mounting plate, on which the fingers are mounted. Each pressure inlet is used to supply pneumatic pressure into the ribbed internal chamber of the finger. Due to similar abbreviations of fluidic elastomer actuator and finite element analysis, the specific configuration of the soft gripper in this study is referred to as soft pneumatic finger. The experimental setup consists of the soft gripper, a base plate and a spherical workpiece (hereinafter referred to as the ball) that is selected as the gripped object. The ball is a solid 50 mm-diameter structural steel spherical object.
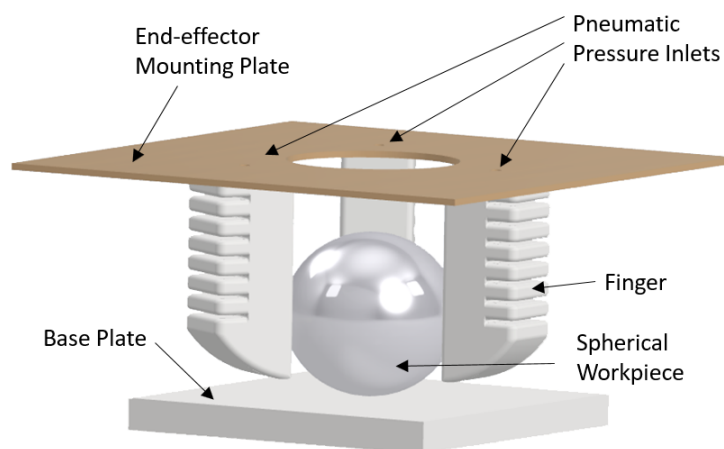
Figure 1. Mechanical design of the soft robotic gripper and experimental setup

2.2. Finger design

The design of the finger is based on a ribbed internal channel design that is commonly used in soft pneumatic fingers [28]. The detailed design of the finger is shown in Figure 2 with all dimensions in mm. The overall dimension of the finger is 62 mm (L) x 20 m (W) x 25 mm (H). Each finger contains an arched end with a 30 mm radius, and bellow-type ribs along the finger. To ensure the right direction of deformation of the finger when pressure is applied, hollow internal chamber is designed with a 1 mm wall thickness. A higher stiffness is achieved by a 5 mm-thick finger base.
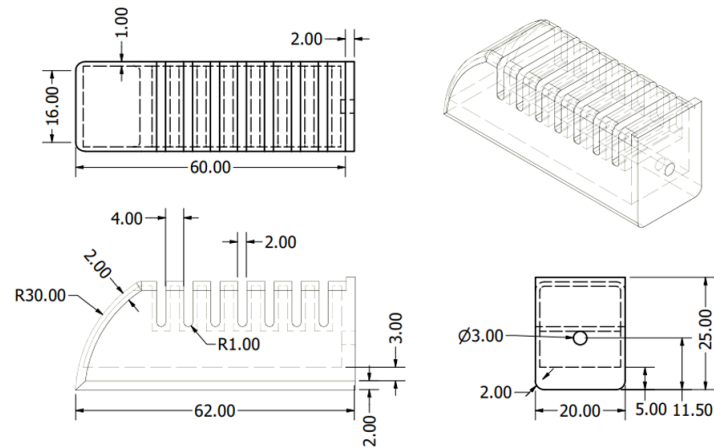
Figure 2. Dimensions of the finger design in mm

2.3. Finger material

Silicone rubber is an elastomer that is widely used for soft robotic fingers, as it can be molded into desired shapes [29] and therefore allows robust manipulation of the grippers. In this study, grade KE-575-U silicone rubber with a density of 1,210 kg/m^3 is taken as a reference as it is used in high strength applications. To account for non-linear stress-strain behavior of the elastomer, Yeoh 3rd order hyperelastic model was selected on Ansys, which was demonstrated by [30] to be suitable for low pressure (190-270 kPa). Thus, this model is selected as most soft pneumatic fingers operate at gauge pressure of below 100 kPa [31],[32]. The stress-strain relationships of the finger material used in the finite element analysis is obtained from Ansys and is shown in Figure 3.
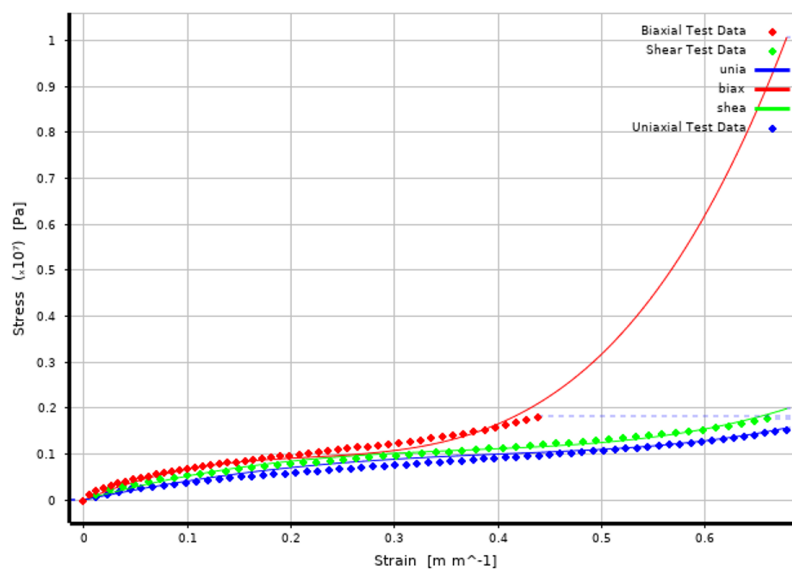
Figure 3. Stress-strain relationships of the silicone rubber used in this study

3. ANSYS SIMULATION METHOD

The Ansys finite element analysis simulation aims to investigate the stress and deformation of the soft fingers when input pneumatic pressure is applied, as well as the stress experienced by the object. It is assumed that the ball's deformation is negligible as compared to the deformation of the fingers. The analysis used in this simulation is Static Structural analysis and it is performed at a temperature of 23°C.

3.1. Contact connections

Contact connections among the objects need to be specified in Ansys. In this setup, the base plate and end-effector mounting plates are fixed. The soft fingers (namely Fingers A, B and C) are bonded to the end-effector mounting plate. The ball is bonded to the base plate. Additionally, the contacts between the fingers and the ball are frictional contacts. A summary of the contacts used in the simulation is shown in Table 1.

Table 1. Contact connections used in the simulation

No.	Contact Object	Target Object	Contact Type
1	Finger A	Mounting Plate	Bonded
2	Finger B	Mounting Plate	Bonded
3	Finger C	Mounting Plate	Bonded
4	Ball	Base Plate	Bonded
5	Finger A	Ball	Frictional
6	Finger B	Ball	Frictional
7	Finger C	Ball	Frictional

3.2. Mesh sizing

A targeted element mesh size of 0.02 mm was applied in conjunction with an aggressive mechanical shape checking. The mesh size is further refined by adaptive sizing. These settings ensure the solver's ability to take into account of large stress and strain values and generate high-quality non-linear solution.

3.3. Input pressure application

The pneumatic actuation of the soft robotic fingers are simulated by applying pressure into the internal chamber of the fingers. Figure 4 shows the selected internal faces for the pressure application. The arrangement of the internal chamber allows for the bending of the finger when input pressure is applied.
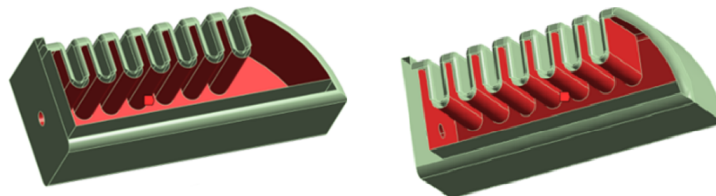
Figure 4. Surface selections for pressure application

4. PARAMETRIC STUDY

Given the finger design and size of the ball, two significant parameters that can be varied to affect the gripping actions are the input pressure as well as the spacing between fingers. In this study, 36 different cases are investigated by varying the input pressure (from 5 kPa to 60 kPa with 5 kPa increment) and the finger radial spacing (measuring from the center of the ball to the nearest surface of the finger). The list of varied parameters and intended simulations is illustrated in Figure 5.

4.1. Non-dimensionalization of finger spacing and object size

The clearance between the fingers and the object depends on the spacing between the fingers and the object size. It is evident that fingers that are spaced further apart are able to grip wider range of object sizes, however, higher input pressure will be necessary to deform the fingers enough to grasp the object. Therefore, by non-dimensionalizing this two parameters may provide more generalized insights on how different parameters come into play. To illustrate this, a bottom view of the fingers and a shperical sample object is shown in Figure 6.
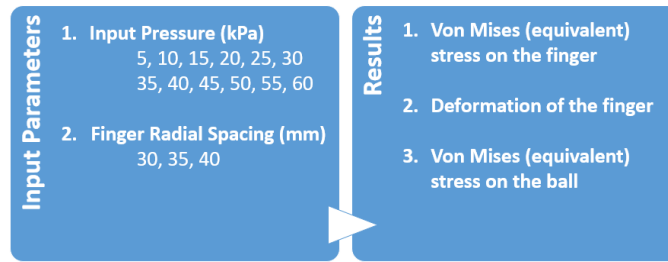
Figure 5. Varied input parameters and investigated results of the parametric study
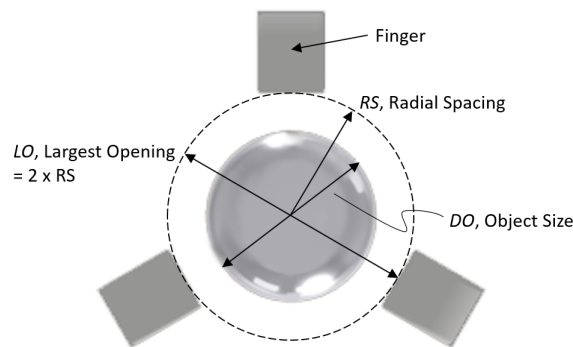
Figure 6. Finger spacing and object size

A non-dimensional parameter, clearance ratio, CR can be developed. Here, the finger radial spacing is denoted as RS and the largest opening of the gripper is therefore $LO = 2$. The object size is denoted as DO. The expression for calculating the clearance ratio is:

$$CR = \frac{LO - DO}{LO} = 1 - \frac{DO}{2RS} \tag{1}$$

Therefore, CR has a physical definition of the clearance between the fingers and the object with respect to object size. A limiting case of $CR = 0$ means that the object size is the same the largest opening of the gripper and a limiting case of $CR = 1$ means that the object size is 0. A larger CR value signifies larger clearance between the fingers and the object. Table 2 shows the CR for different finger spacings.

Table 2. Clearance ratios for different finger spacings

Radial spacing RS (mm)	Largest opening LO (mm)	Object size DO (mm)	Clearance ratio CR
30	60	50	16.67%
35	70	50	28.57%
40	80	50	37.50%

4.2. Total deformation

In Ansys, total deformation refers to the displacements caused by stress and it is a scalar value that is calculated by taking the Euclidean distance between its initial location and displaced location. The deformation of the soft fingers is a useful parameter to investigate as the deformation itself is the result of actuating input pressure and it determines if the object is successfully grasped by the fingers. As the gripped object is assumed to be rigid, its deformation is much lesser than the deformation of the fingers and therefore is not of interest to be investigated.

4.3. Von Mises (equivalent) stress

The Von Mises stress measures the equivalent stress on the three principal axes. The Von Mises stress is commonly used to predict material yielding and determine the yield factor of safety for ductile materials. This simulated parameter is chosen as elastomers are ductile materials.

5. RESULTS AND DISCUSSION

The gripping simulation of the ball is performed by applying different input pressures and clearance ratios as shown Figure 5 and Table 2. To investigate how much stress and deformation are developed on the soft fingers and how much stress is developed on the ball, the Static Ball experiment is conducted by restraining all objects from moving, except for the fingers.

5.1. Static ball - total deformation of the finger

The simulation result of the gripper's total deformation when 60 kPa is applied to gripper with finger radial spacing of 40 mm (CR=37.50%) is shown in Figure 7. An isolated view of a single finger is shown in Figure 8. At zero pressure, the opening of the gripper is 80 mm and assuming that all three fingers experience identical deformations, the further point of the finger should deform by $CR = (LO - DO)/2$=15 mm or more toward the center of the ball in order to establish contact with the ball. It can be seen that in this setup, the total deformation of the finger is 21.418 mm, which occurs near the tip of the finger. Visually, Figure 7 shows that the fingers are making physical contacts with the ball.
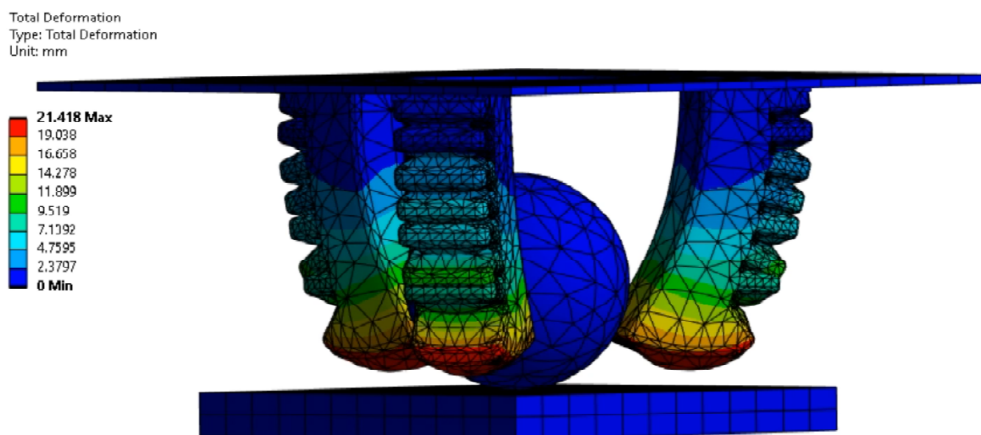
Figure 7. Total deformation of the gripper at 60 kPa input pressure and finger radial spacing of 4.0 mm (CR=37.50%). The ball is fixed to the base plate
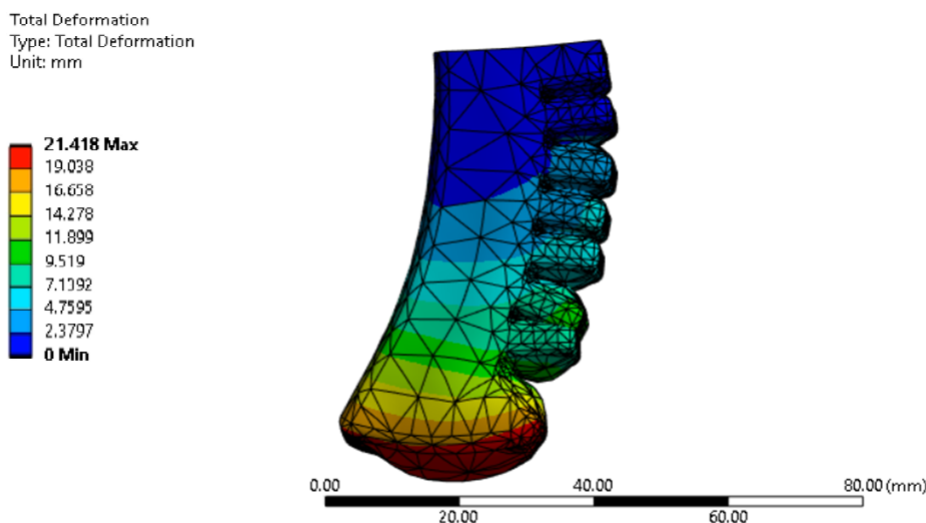
Figure 8. Total deformation of a single soft finger at 60 kPa input pressure and finger radial spacing of 4.0 mm (CR=37.50%)

The average total deformation of the finger for different cases is shown in Figure 9. The average total deformation measures the average of total deformations of all the nodes. It can be seen that for an input pressure of 15 kPa and below, the average total deformation for three different finger spacings are the same, and that the deformation and input pressure relationships are linear. This is due to the fact that none of fingers has made contacts with the ball.

Given that the applied input pressure is varied by an increment of 5 kPa, it can be observed that for CR=16.67%, the contact with the ball happens at 20 kPa and above. Contacts with the ball happen starting at 35 kPa and 45kPa for CR=28.57% and CR=37.50%, respectively. It can be concluded that the average total deformations of the fingers are higher for higher CR and finger spacings once the fingers are in contact with the ball.
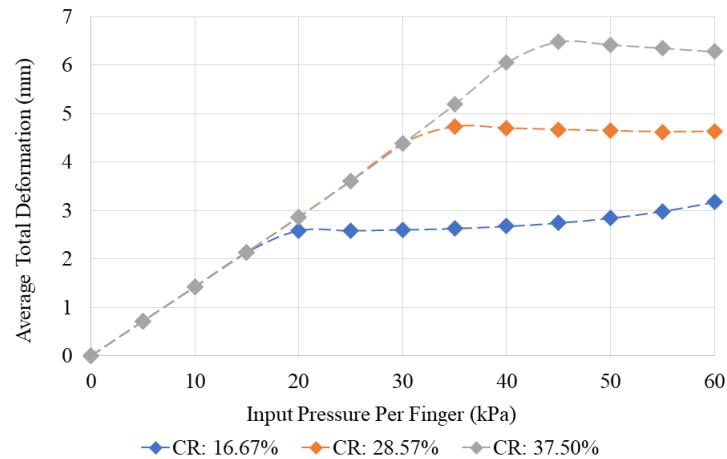
Figure 9. Average total deformation of the finger for different input pressures and clearance ratios

5.2. Static ball - Von Mises (equivalent) stress on the finger

The equivalent stress experienced by the finger when 60 kPa is applied to gripper with finger radial spacing of 40 mm (CR=37.50%) is shown in Figure 10. Visually, it can be seen that most nodes experience equivalent stress of lesser than 1MPa although the reported maximum equivalent stress is at 6.4365MPa and it occurs at the most bottom trough of the ribs. This offers a valuable insight when designing internal chamber of the finger as it shows the locations of where stress concentration may occur and how revisions in design may mitigate it.
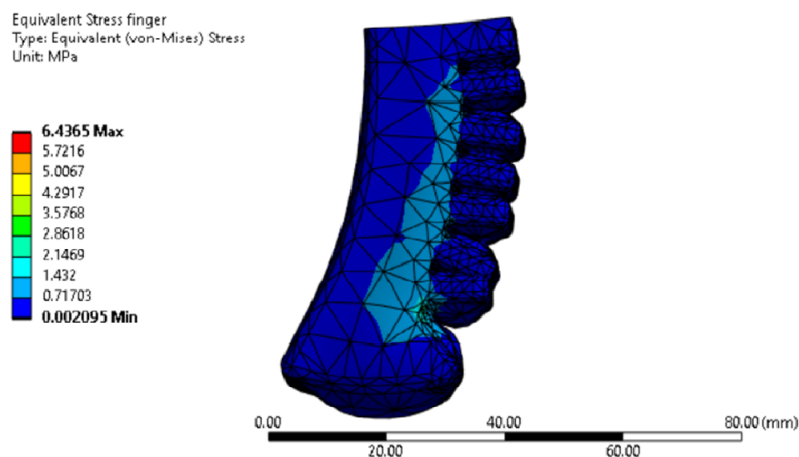
Figure 10. Von Mises (equivalent) stress of a single soft finger at 60 kPa input pressure and finger radial spacing of 4.0mm (CR=37.50%)

The average equivalent stress experienced by the finger for different cases is shown in Figure 11. The average equivalent stress measures the average of equivalent stress of all the nodes. There is no significant difference for the three finger spacings, although, at given input pressure, a gripper with larger finger spacing develops larger equivalent stress as compared to those with smaller finger spacings.
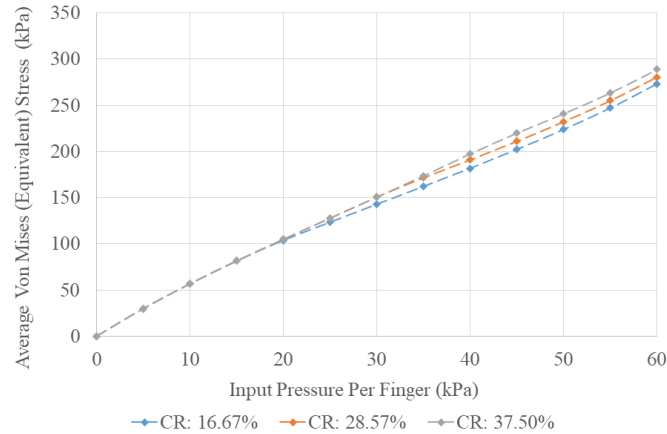
Figure 11. Average Von Mises (equivalent) stress on the finger for different input pressures and clearance ratios

5.3. Static ball - Von Mises (equivalent) stress on the ball

The equivalent stress experienced by the ball when 60 kPa is applied to gripper with finger radial spacing of 40 mm (CR=37.50%) is shown in Figure 12. It can be seen that most nodes experience equivalent stress of lesser than 1kPa with the reported maximum equivalent stress of 16.307 kPa and it occurs at the points of contact with the fingers. The average equivalent stress of the ball for different cases is shown in Figure 13. Here, the average equivalent stress of 0 implies that the ball is not in contact with the fingers and hence no stress is developed (for static ball experiment, the ball is bonded with the baseplate).
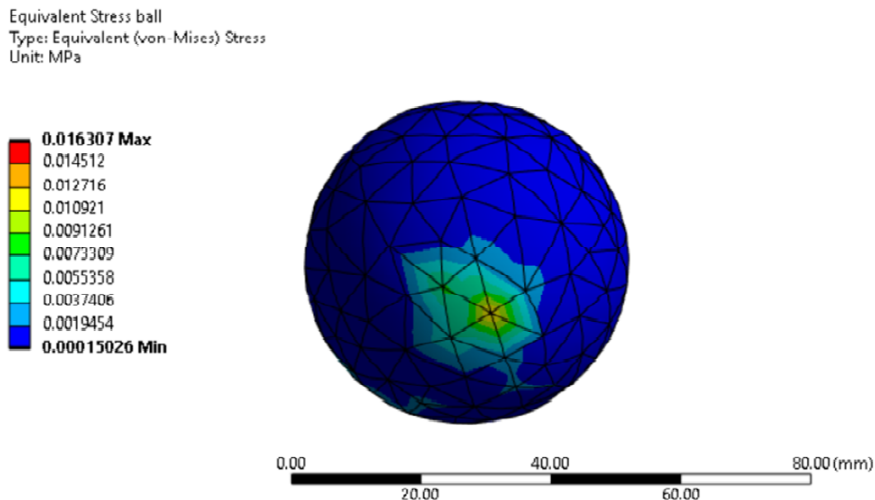
Figure 12. Von Mises (equivalent) stress of the ball at 60 kPa input pressure and finger radial spacing of 4.0 mm (CR=37.50%)

This finding is consistent with the input pressures discussed in subsection 5.1, where for CR=16.67%, the contact with the ball happens at 20kPa and above. For CR=28.57% and CR=37.50%, the contacts with the ball happen starting at 35kPa and 45kPa, respectively. It is also observed that for smaller

finger spacing, the equivalent stress experienced by the ball for a given input pressure is higher. This means that the grippers with lower CR produces better gripping.
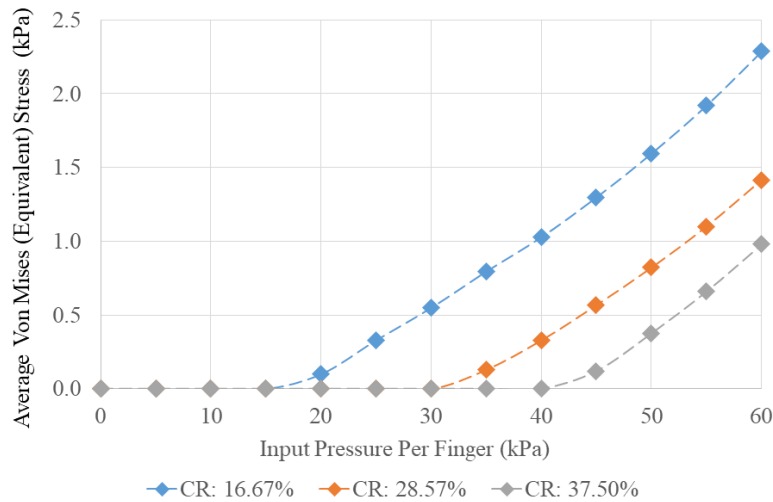
Figure 13. Average Von Mises (equivalent) stress on the ball for different input pressures and clearance ratios

5.4. Lifting ball

The static ball experiment allows the analysis of how well the soft gripper is able to grip the object as well as the identification of stress concentrations on the fingers, which may be used to improve the design of the soft finger. The lifting ball experiment discussed below is conducted to verify that a set of given input pressure and selected finger spacing is able to lift the ball. The only difference between the static ball experiment and lifting ball experiment is that the ball is not bonded to the base plate and therefore is allowed to move as a result of physical contacts with the fingers.

A starting case to make contact with the ball, with input pressure of 20 kPa with finger radial spacing of 30 mm (CR=16.67%), is simulated for the Lifting Ball experiment. The total deformation simulation result is shown in Figure 14. The ball is successfully lifted up, while the fingers experience maximum deformation of 8.3448 mm.
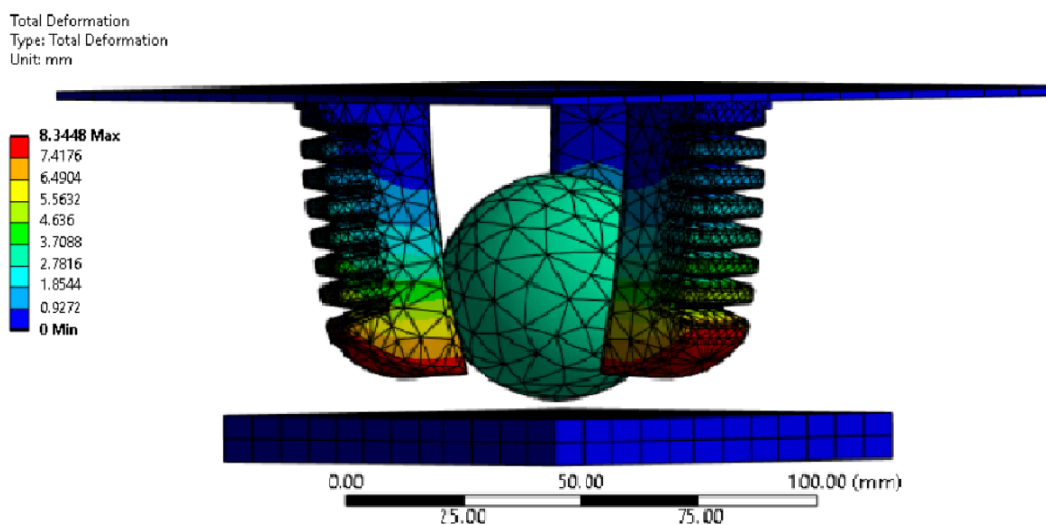
Figure 14. Total deformation of the gripper and the ball at 20 kPa input pressure and finger radial spacing of 3.0mm (CR=16.67%) for lifting ball experiment

The reported total deformation of the ball signifies how much a node in the ball has displaced as opposed to how much the ball has deformed. This is due to the fact that the static structural analysis of ansys calculates deformation as the displacement of a node location. For the case of an unbonded object, the displacement of the node is caused by both motion and deformation at the same time. The average deformation of the ball is 3.2378 mm, which gives an indication of the displacement of the ball from its initial location. The equivalent stress experienced by the finger is shown in Figure 15. It is seen that the maximum equivalent stress on the finger is 498.69kPa and the average equivalent stress on the finger is 104.96 kPa.
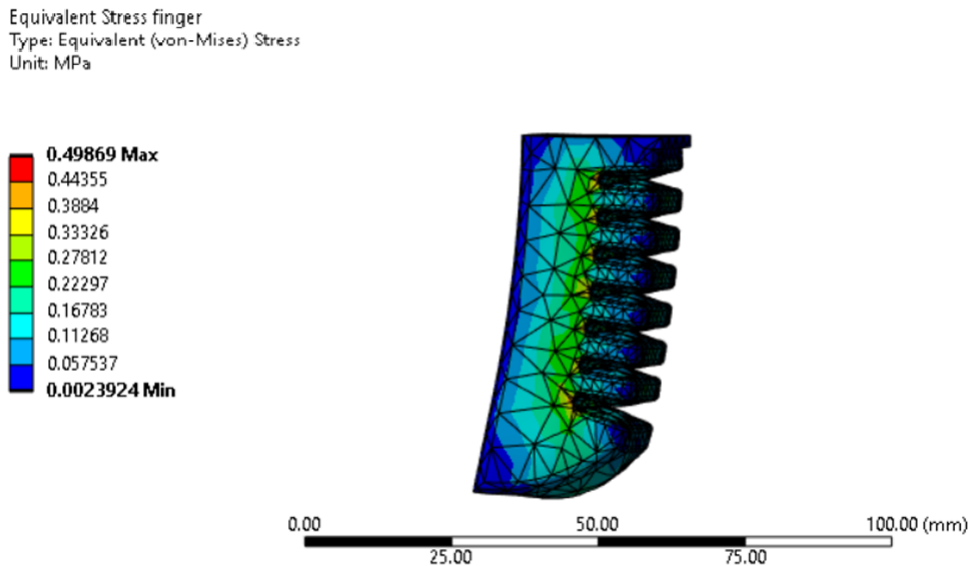
Figure 15. Von Mises (equivalent) stress of the ball at 20kPa input pressure and finger radial spacing of 3.0mm (CR=16.67%) for lifting ball experiment

6.   CONCLUSION AND FUTURE WORKS

This paper presents a parametric study of pneumatically-actuated soft robotic fingers by considering elastomer properties, finger spacing and input pressure. Results presented provide insights in optimizing the design of soft robotic grippers, i.e. design against stress concentration and choosing the compromise between graspable range and input pressure. Future works include extending the parametric study to consider more parameters, such as temperature that may affect the properties of the elastomer, variations in the designs and sizes of the fingers as well as object shapes. Prototype development can also be performed to validate the simulation results.

ACKNOWLEDGEMENT

REFERENCES

[1] A. Gasparetto and L. Scalera, "From the unimate to the delta robot: The early decades of industrial robotics," in *History of Mechanism and Machine Science*, 2019, vol. 37, pp. 284–295, doi: 10.1007/978-3-030-03538-9_23.
[2] Z. Zhang, A. Pan, X. Li, and Y. Luo, "Large-model and generative-intelligence agricultural robot systems," in *2023 International Annual Conference on Complex Systems and Intelligent Science (CSIS-IAC)*, Oct. 2023, pp. 752–759, doi: 10.1109/CSIS-IAC60628.2023.10363912.
[3] K. T. Chew, R. S. Jo, M. Lu, V. Raman, and P. H. Hui Then, "Organic black soldier flies (BSF) farming in rural area using libelium waspmote smart agriculture and internet-of-things technologies," in *IEEE 11th Symposium on Computer Applications and Industrial Electronics*, 2021, pp. 228–232, doi: 10.1109/ISCAIE51753.2021.9431801.

[4]   Z. Al-Mashhadani and J. H. Park, "Autonomous agricultural monitoring robot for efficient smart farming," in *International Conference on Control, Automation and Systems*, 2023, pp. 640–645, doi: 10.23919/ICCAS59377.2023.10316866.

[5]   Z. Wang, K. Or, and S. Hirai, "A dual-mode soft gripper for food packaging," *Robotics and Autonomous Systems*, vol. 125, 2020, doi: 10.1016/j.robot.2020.103427.

[6]   A. Stepanova, H. Pham, and A. Zourmand, "Robotics solution for agriculture: automated and IoT-enabled tomato picking and packing," in *2023 IEEE International Conference on Agrosystem Engineering, Technology and Applications*, 2023, pp. 108–112, doi: 10.1109/AGRETA57740.2023.10262632.

[7]   E. Drijver, R. Pérez-Dattari, J. Kober, C. Della Santina, and Z. Ajanovic, "Robotic packaging optimization with reinforcement learning," in *IEEE International Conference on Automation Science and Engineering*, 2023, pp. 1–7, doi: 10.1109/CASE56687.2023.10260406.

[8]   S. Hirose and Y. Umetani, "The development of soft gripper for the versatile robot hand," *Mechanism and Machine Theory*, vol. 13, no. 3, pp. 351–359, 1978, doi: 10.1016/0094-114X(78)90059-9.

[9]   J. Shintake, V. Cacucciolo, D. Floreano, and H. Shea, "Soft robotic grippers," Advanced *Materials*, vol. 30, no. 29, 2018, doi: 10.1002/adma.201707035.

[10]   S. Li *et al.*, "JamTac: a tactile jamming gripper for searching and grasping in low-visibility environments," *Soft Robotics*, vol. 10, no. 5, pp. 988–1000, 2023, doi: 10.1089/soro.2022.0134.

[11]   M. B. Schafer, J. H. Friedrich, J. Hotz, L. Worbs, S. Weiland, and P. P. Pott, "Robotic scrub nurse: surgical instrument handling with a granular jamming gripper," *Current Directions in Biomedical Engineering*, vol. 9, no. 1, pp. 174–177, 2023, doi: 10.1515/cdbme-2023-1044.

[12]   J. Hu, L. Liang, and B. Zeng, "Design, modeling, and testing of a soft actuator with variable stiffness using granular jamming," *Robotica*, vol. 40, no. 7, pp. 2503–2503, Jul. 2022, doi: 10.1017/S0263574722000315.

[13]   D. Howard, J. O'Connor, J. Brett, and G. W. Delaney, "Shape, size, and fabrication effects in 3D printed granular jamming grippers," in *2021 IEEE 4th International Conference on Soft Robotics*, 2021, pp. 458–464, doi: 10.1109/RoboSoft51838.2021.9479438.

[14]   E. Brown *et al.*, "Universal robotic gripper based on the jamming of granular material," in *Proceedings of the National Academy of Sciences of the United States of America*, vol. 107, no. 44, pp. 18809–18814, 2010, doi: 10.1073/pnas.1003250107.

[15]   H. Baek, A. M. Khan, V. Bijalwan, S. Jeon, and Y. Kim, "Dexterous robotic hand based on rotational shape memory alloy actuator-joints," *IEEE Transactions on Medical Robotics and Bionics*, vol. 5, no. 4, pp. 1082–1092, 2023, doi: 10.1109/TMRB.2023.3315783.

[16]   K. Hyeon, C. Chung, J. Ma, and K. U. Kyung, "Lightweight and flexible prosthetic wrist with shape memory alloy (SMA)-based artificial muscle and elliptic rolling joint," *IEEE Robotics and Automation Letters*, vol. 8, no. 11, pp. 7849–7856, 2023, doi: 10.1109/LRA.2023.3320496.

[17]   W. Wang and S. H. Ahn, "Shape memory alloy-based soft gripper with variable stiffness for compliant and effective grasping," *Soft Robotics*, vol. 4, no. 4, pp. 379–389, 2017, doi: 10.1089/soro.2016.0081.

[18]   A. Hajj-Ahmad, L. Kaul, C. Matl, and M. Cutkosky, "GRASP: grocery robot's adhesion and suction picker," *IEEE Robotics and Automation Letters*, vol. 8, no. 10, pp. 6419–6426, 2023, doi: 10.1109/LRA.2023.3300572.

[19]   W. Ruotolo, D. Brouwer, and M. R. Cutkosky, "From grasping to manipulation with gecko-inspired adhesives on a multifinger gripper," *Science Robotics*, vol. 6, no. 61, 2021, doi: 10.1126/scirobotics.abi9773.

[20]   J. A. Sandoval, T. Xu, I. Adibnazari, D. D. Deheyn, and M. T. Tolley, "Combining suction and friction to stabilize a soft gripper to shear and normal forces, for manipulation of soft objects in wet environments," *IEEE Robotics and Automation Letters*, vol. 7, no. 2, pp. 4134–4141, 2022, doi: 10.1109/LRA.2022.3149306.

[21]   S. A. Suresh, A. Hajj-Ahmad, E. W. Hawkes, and M. R. Cutkosky, "Forcing the issue: testing gecko-inspired adhesives," *Journal of The Royal Society Interface*, vol. 18, no. 174, Jan. 2021, doi: 10.1098/rsif.2020.0730.

[22]   Z. Gao *et al.*, "Electrically controlled underwater object manipulation with adhesive borate ester hydrogels," *Materials Today Nano*, vol. 24, 2023, doi: 10.1016/j.mtnano.2023.100396.

[23]   E. W. Schaler, D. Ruffatto, P. Glick, V. White, and A. Parness, "An electrostatic gripper for flexible objects," in *IEEE International Conference on Intelligent Robots and Systems*, 2017, pp. 1172–1179, doi: 10.1109/IROS.2017.8202289.

[24]   J. Poccard-Saudart, S. Xu, C. B. Teeple, N. S. P. Hyun, K. P. Becker, and R. J. Wood, "Controlling soft fluidic actuators using soft DEA-based valves," *IEEE Robotics and Automation Letters*, vol. 7, no. 4, pp. 8837–8844, 2022, doi: 10.1109/LRA.2022.3187268.

[25]   Y. Wu *et al.*, "A bioinspired multi-knuckle dexterous pneumatic soft finger," *Sensors and Actuators A: Physical*, vol. 350, 2023, doi: 10.1016/j.sna.2022.114105.

[26]   Y. Wu, M. Lu, L. Ding, and T. Zhong, "Design and motion analysis of a bidirectional parallel-chamber soft pneumatic actuator," in *Proceedings of the Institution of Mechanical Engineers, Part C: Journal of Mechanical Engineering Science*, Dec. 2023, doi: 10.1177/09544062231210079.

[27]   Y. Zhuang *et al.*, "Analysis of mechanical characteristics of stereolithography soft-picking manipulator and its application in grasping fruits and vegetables," *Agronomy*, vol. 13, no. 10, 2023, doi: 10.3390/agronomy13102481.

[28]   A. D. Marchese, R. K. Katzschmann, and D. Rus, "A recipe for soft fluidic elastomer robots," *Soft Robotics*, vol. 2, no. 1, pp. 7–25, 2015, doi: 10.1089/soro.2014.0022.

[29]   C. H. Liu *et al.*, "Optimal design of a soft robotic gripper for grasping unknown objects," *Soft Robotics*, vol. 5, no. 4, pp. 452–465, 2018, doi: 10.1089/soro.2017.0121.

[30]   C. S. Ying, J. L. S. Ern, and F. W. Y. Myan, "Numerical investigation on two-wheeler bias tyre impact using various material models," *Journal of Engineering Science and Technology*, vol. 13, pp. 92–103, 2018.

[31]   R. Gao, J. Fang, J. Qiao, C. Li, and L. Zhang, "The bending control of the soft pneumatic finger," in *Journal of Physics: Conference Series*, 2022, vol. 2181, no. 1, doi: 10.1088/1742-6596/2181/1/012060.

[32]   K. Batsuren and D. Yun, "Soft robotic gripper with chambered fingers for performing in-hand manipulation," *Applied Sciences*, vol. 9, no. 15, Jul. 2019, doi: 10.3390/app9152967.

BIOGRAPHIES OF AUTHORS

Riady S. Jo ⓘ 🗺 🆂🅲 ◖ is an Associate Professor at the School of Engineering and Technology, Sunway University, Malaysia. He holds Bachelor of Engineering in Robotics and Mechatronics and PhD in Engineering from Swinburne University of Technology, Australia. Riady is a former Assistant Professor and Deputy Programme Director of Studies of Mechanical Engineering at Heriot-Watt University Malaysia and former Lecturer at Swinburne University of Technology Sarawak Campus, Malaysia. His research interest include engineering education, robotics, automation, control systems and internet-of-things applications. He can be contacted at email: riadyj@sunway.edu.my.

Evans Ngu ⓘ 🗺 🆂🅲 ◖ currently pursues a Master of Engineering in Mechanical Engineering, Heriot-Watt University, United Kingdom. Prior to his transfer to the United Kingdom, Evans undertook his Master's study in Heriot-Watt University Malaysia. His interests include mechanical system design and finite element analysis. He can be contacted at email: en33@hw.ac.uk.